Cavity as a source of conformational fluctuation and high-energy state: High-pressure NMR study of a cavity-enlarged mutant of T4 lysozyme

Akihiro Maeno, Daniel Sindhikara, Fumio Hirata, Renee Otten, Frederick W. Dahlquist, Shigeyuki Yokoyama, Kazuyuki Akasaka, Frans A. A. Mulder, and Ryo Kitahara

Contents: Methods and Fig. S1-S7

Methods

RISM theory

3D-RISM is a computational solvent representation that is based on statistical liquid theory (1,2). We briefly review the equations below, as they have already been discussed in detail elsewhere (3,4). The 3D-RISM equation is given by:

$$h_\gamma^{uv}(\vec{r}) = \sum_{v' \in V} \sum_{\alpha \epsilon v'} c_\alpha^{uv'} * \left[\omega_{\alpha\gamma}^{v'v} + \rho^{v'} h_{\alpha\gamma}^{v'v}\right](\vec{r}) \qquad (1)$$

where here *h*, *c*, and ω are the total, direct and intramolecular correlation functions, respectively, and the asterisk denotes the convolution integrals. ρ^v is the average density of solvent species, whereas *v*, γ, and α represent the solvent site of interest and reference site, respectively The term *V* represents all of the solvent species, whereas *u* and *v* represent the sites contained in the solute and solvent, respectively. In order to close the above equation, we choose the Kovalenko-Hirata closure (5):

$$g_\gamma^{uv}(\vec{r}) = \begin{cases} exp\left(d_\gamma^{uv}(\vec{r})\right) & for \quad d_\gamma^{uv}(\vec{r}) \leq 0 \\ 1 + d_\gamma^{uv}(\vec{r}) & for \quad d_\gamma^{uv}(\vec{r}) > 0 \end{cases} \qquad (2)$$

$$g_\gamma^{uv}(\vec{r}) = h_\gamma^{uv}(\vec{r}) + 1$$

$$d_\gamma^{uv}(\vec{r}) = -\beta U_\gamma^{uv}(\vec{r}) + h_\gamma^{uv}(\vec{r}) - c_\gamma^{uv}(\vec{r})$$

where

$$U_\gamma^{uv}(\vec{r}) = \sum_{\alpha \in u} U_{\gamma\alpha}^{MM,NB}(\vec{r}\text{-}\vec{r}_{alpha})$$

where γ is the distribution function; β, the inverse temperature; and $U^{MM,NB}$, the atomic distance-dependent non-bonded molecular mechanics interaction potential used in typical simulations.

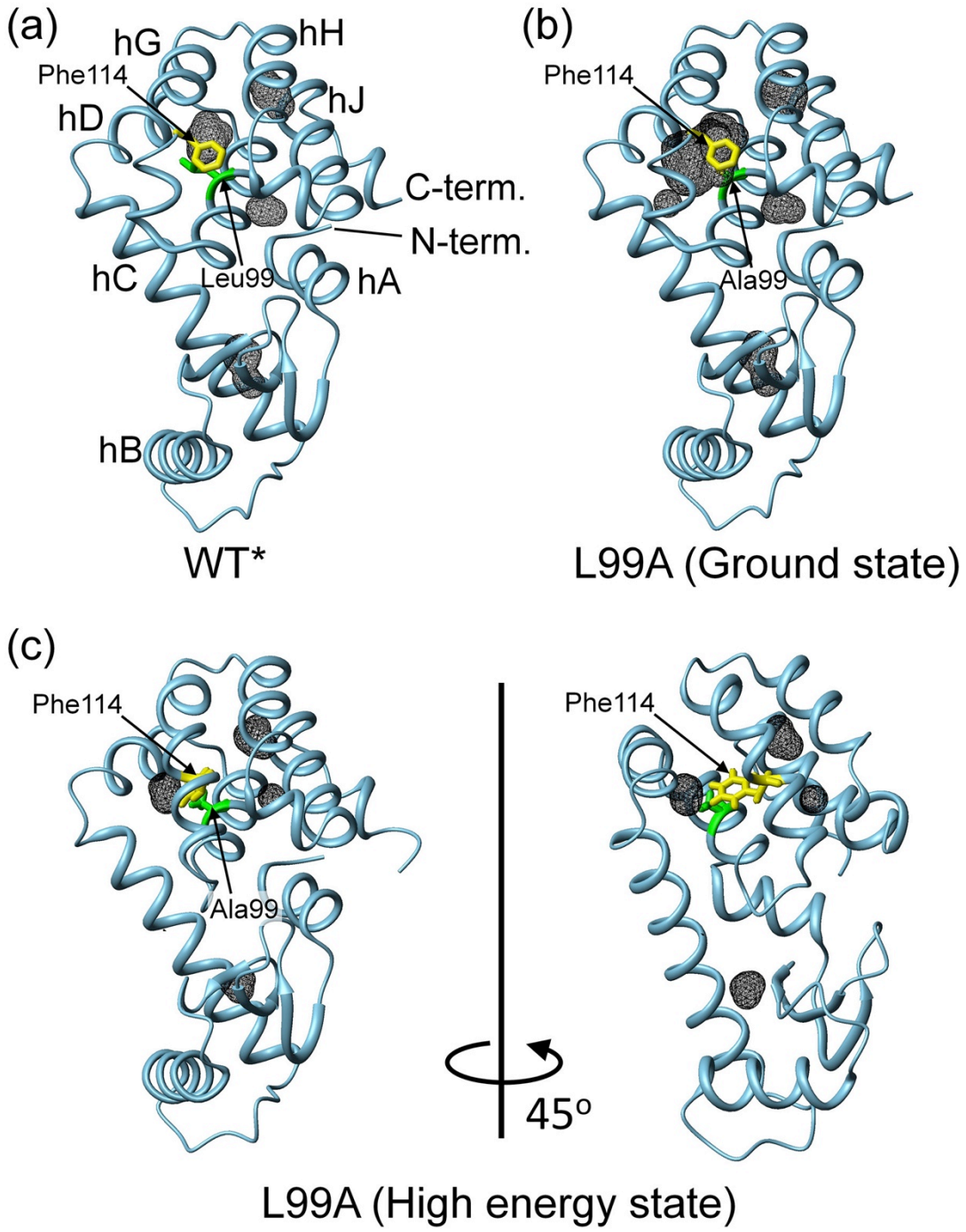

Fig. S1. Three-dimensional structure of T4 lysozyme, (*a*) the pseudo wild-type WT* (PDB ID: 6LZM) and (*b*) L99A (PDB ID: 1L90), and (*c*) L99A high-energy state (PDB ID: 2LCB). Internal cavities are represented by black wire-frame cages calculated by a program MOLMOL with a probe radius of 1.4 Å. Residues 99 and 114 are indicated by stick representations.

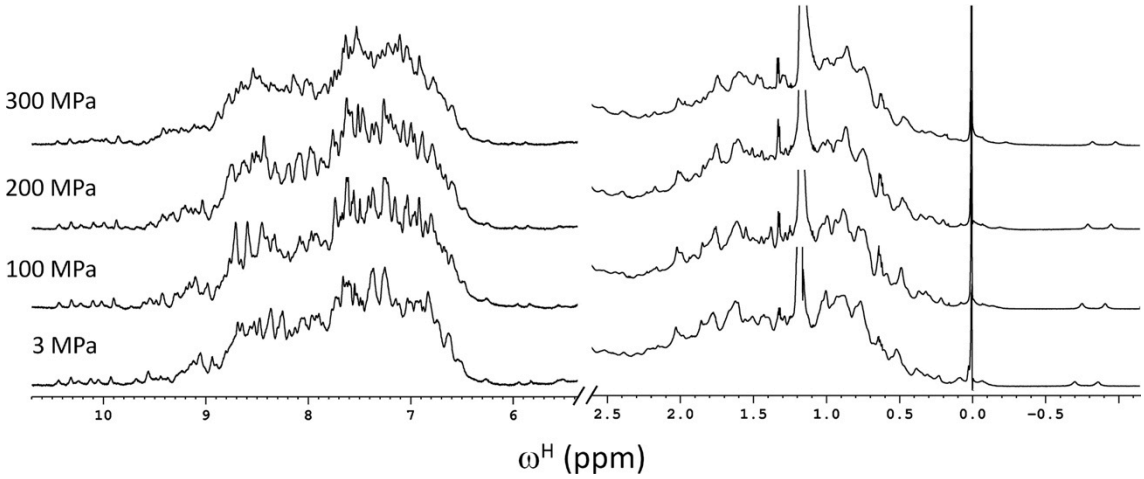

Fig. S2. One-dimensional ^{1}H NMR spectra of uniformly ^{15}N/^{13}C-labeled L99A protein at different pressures from 3 to 300 MPa at 25 ^{o}C. NMR peaks from protons attached to ^{13}C or ^{15}N are split due to J-coupling.

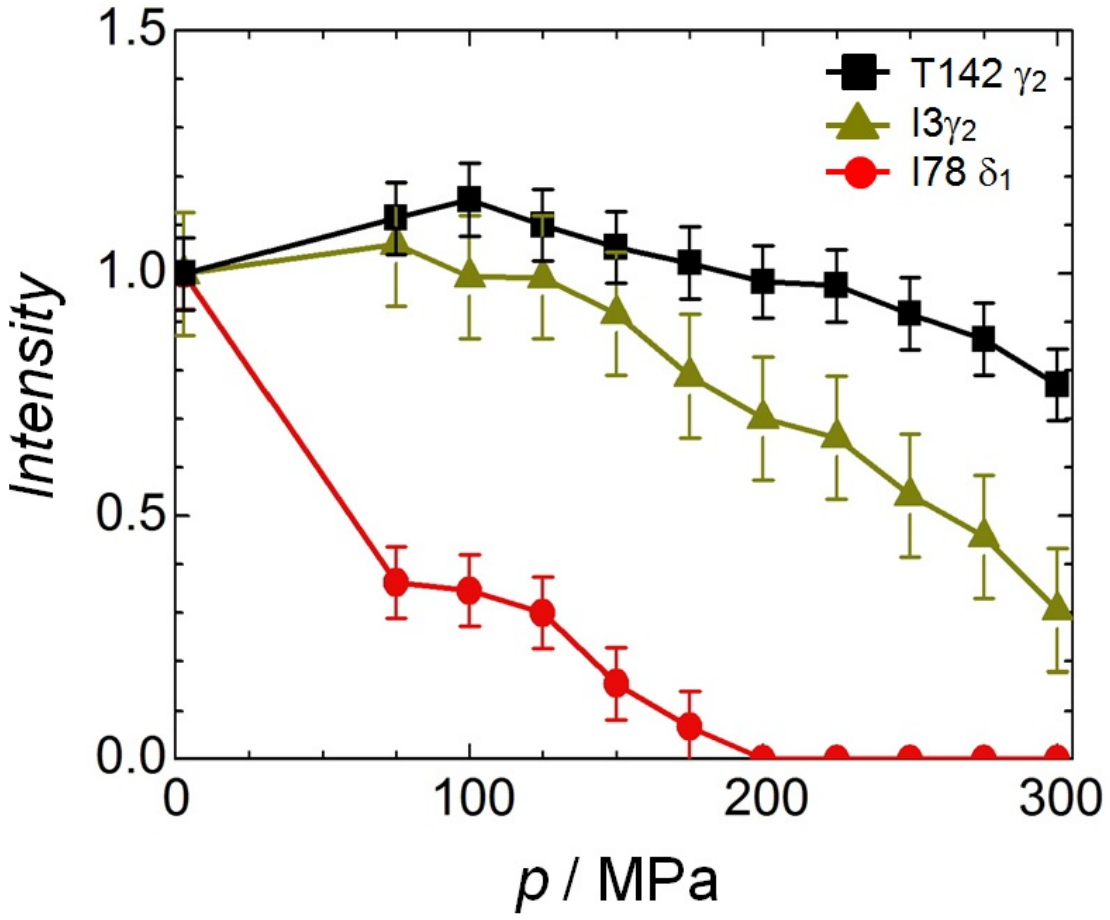

Fig. S3. Errors in peak intensity (i.e. maximum peak height) estimation for representative methyl groups, T142γ_2, I3γ_2, and I78δ_1, which belong to the slow, intermediate, and rapidly decaying groups, respectively (see Fig. 2). Error bars shows the standard deviation of the noise, relative to the signal intensity at 3 MPa.

(a)

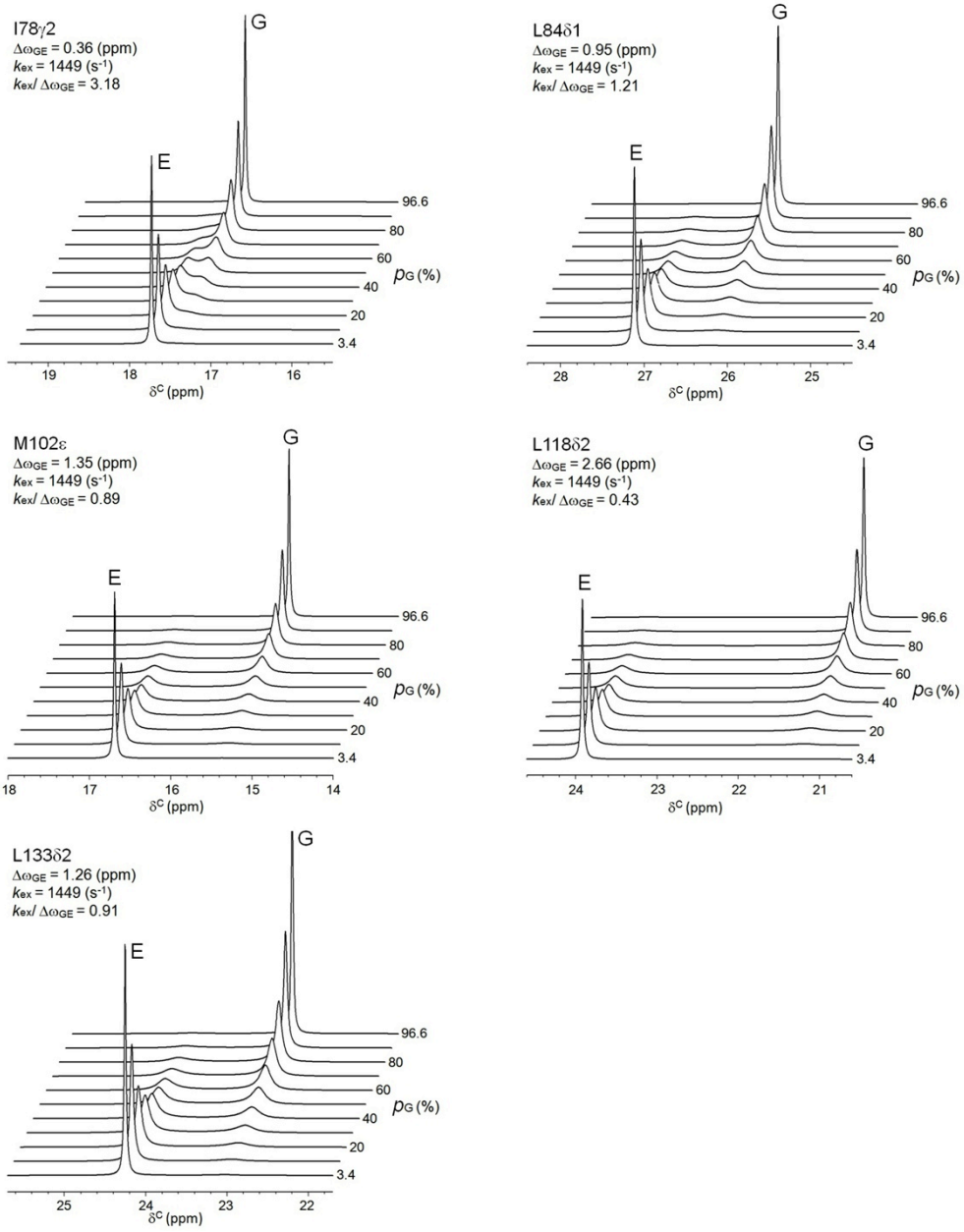
I78γ2
Δω_GE = 0.36 (ppm)
k_ex = 1449 (s-1)
k_ex/ Δω_GE = 3.18
L84δ1
Δω_GE = 0.95 (ppm)
k_ex = 1449 (s-1)
k_ex/ Δω_GE = 1.21
M102ε
Δω_GE = 1.35 (ppm)
k_ex = 1449 (s-1)
k_ex/ Δω_GE = 0.89
L118δ2
Δω_GE = 2.66 (ppm)
k_ex = 1449 (s-1)
k_ex/ Δω_GE = 0.43
L133δ2
Δω_GE = 1.26 (ppm)
k_ex = 1449 (s-1)
k_ex/ Δω_GE = 0.91
G
E
96.6
80
60
40
20
3.4
p_G (%)
δ^C (ppm)

(b)

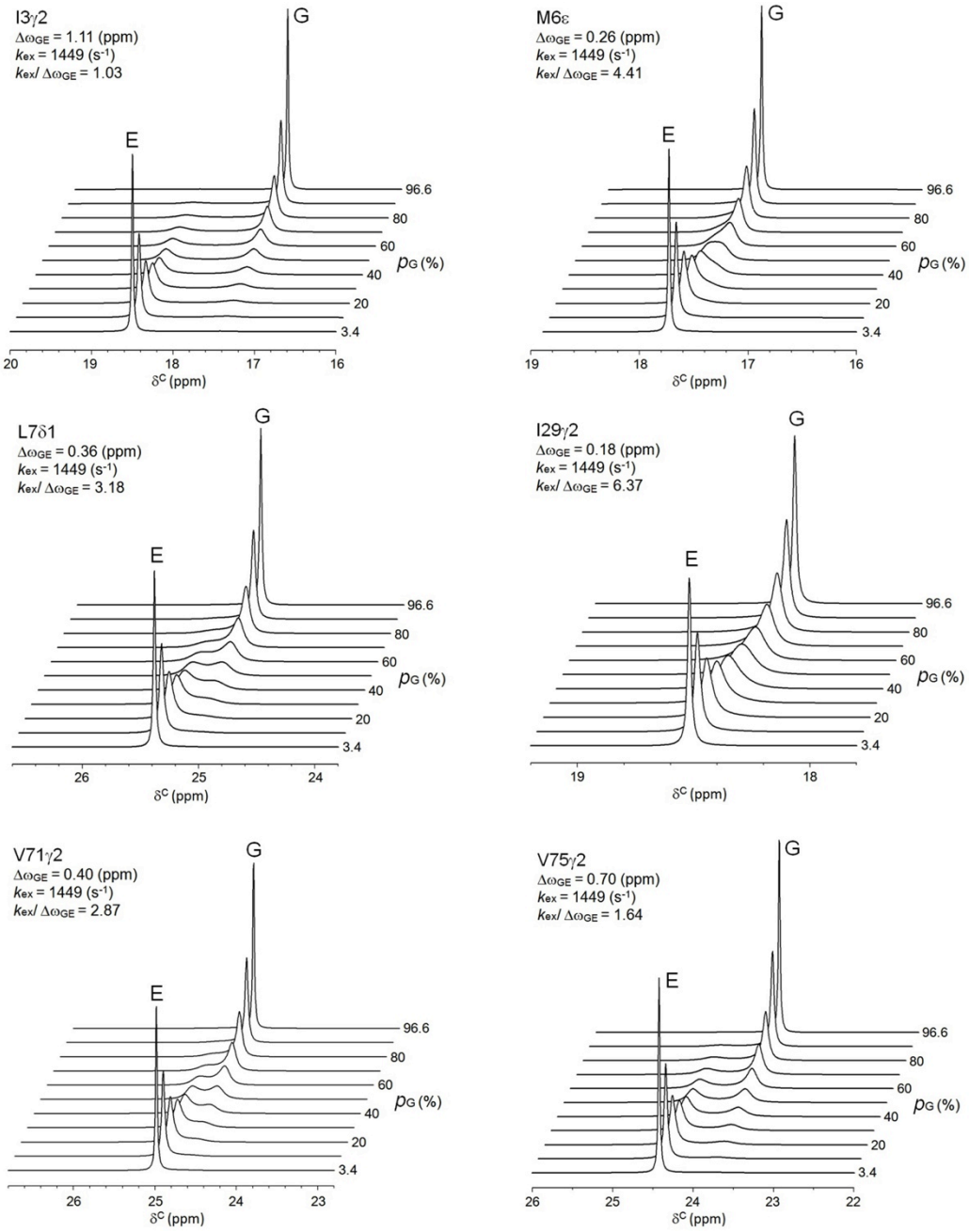
I3γ2
Δω_GE = 1.11 (ppm)
k_ex = 1449 (s⁻¹)
k_ex/ Δω_GE = 1.03
M6ε
Δω_GE = 0.26 (ppm)
k_ex = 1449 (s⁻¹)
k_ex/ Δω_GE = 4.41
L7δ1
Δω_GE = 0.36 (ppm)
k_ex = 1449 (s⁻¹)
k_ex/ Δω_GE = 3.18
I29γ2
Δω_GE = 0.18 (ppm)
k_ex = 1449 (s⁻¹)
k_ex/ Δω_GE = 6.37
V71γ2
Δω_GE = 0.40 (ppm)
k_ex = 1449 (s⁻¹)
k_ex/ Δω_GE = 2.87
V75γ2
Δω_GE = 0.70 (ppm)
k_ex = 1449 (s⁻¹)
k_ex/ Δω_GE = 1.64
G
E
96.6
80
60
40
20
3.4
p_G (%)
δ^C (ppm)

(b)

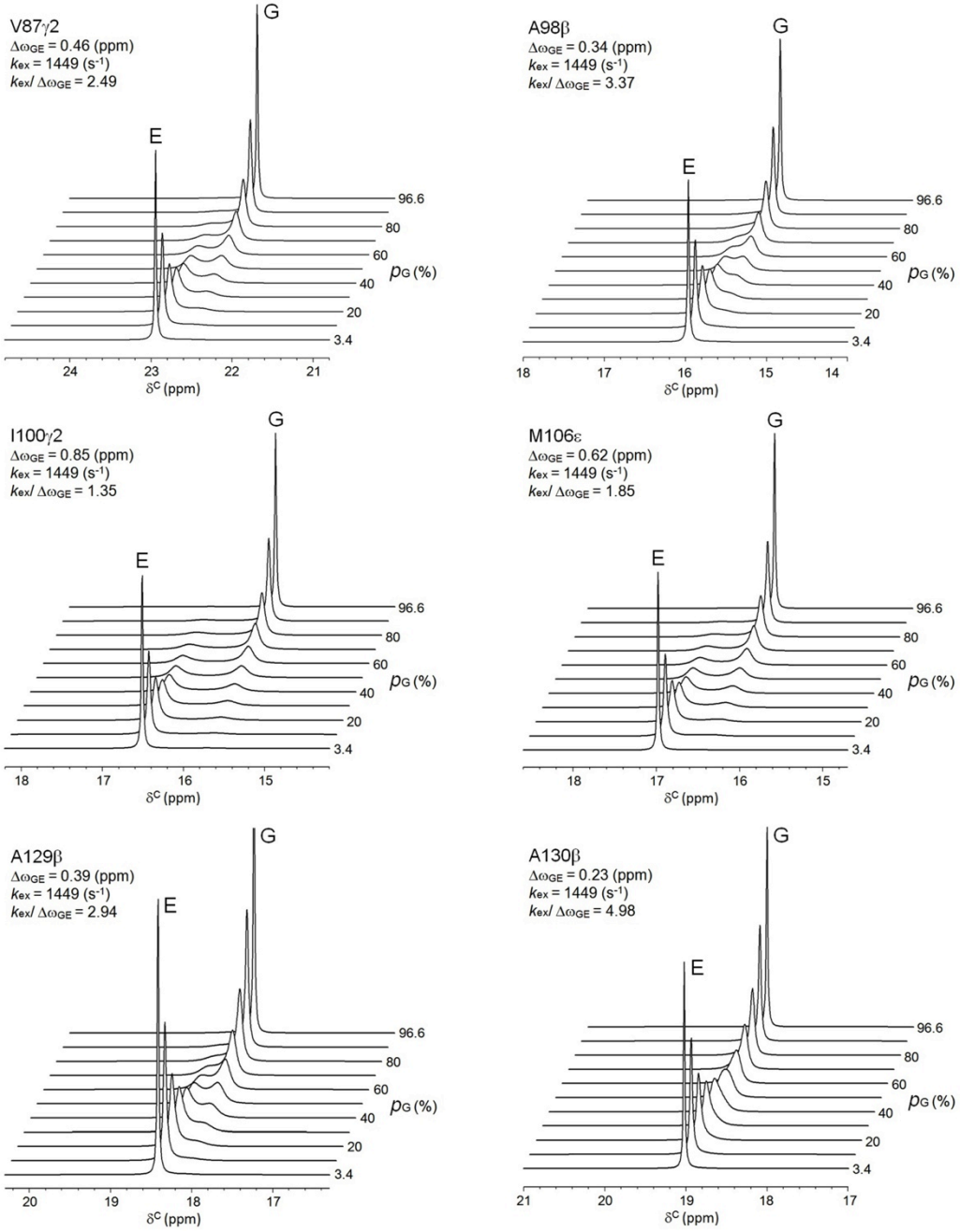
V87γ2
ΔωGE = 0.46 (ppm)
kex = 1449 (s-1)
kex/ ΔωGE = 2.49
A98β
ΔωGE = 0.34 (ppm)
kex = 1449 (s-1)
kex/ ΔωGE = 3.37
I100γ2
ΔωGE = 0.85 (ppm)
kex = 1449 (s-1)
kex/ ΔωGE = 1.35
M106ε
ΔωGE = 0.62 (ppm)
kex = 1449 (s-1)
kex/ ΔωGE = 1.85
A129β
ΔωGE = 0.39 (ppm)
kex = 1449 (s-1)
kex/ ΔωGE = 2.94
A130β
ΔωGE = 0.23 (ppm)
kex = 1449 (s-1)
kex/ ΔωGE = 4.98
G
E
96.6
80
60
40
20
3.4
pG (%)
δC (ppm)

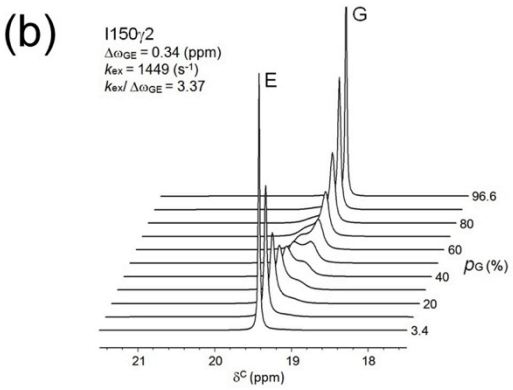

Fig. S4. Line-shape simulation for the methyl carbons of L99A involved in (*a*) the rapidly decaying group (e.g. I78γ_2, L84δ_1, M102ε, L118δ_2 and L133δ_2) and (*b*) the intermediate decaying group (e.g. I3γ_2, M6ε, L7δ_1, I29γ_2, V71γ_2, V75γ_2, V87γ_2, A98β, I100γ_2, M106ε, A129β, A130β, and I150γ_2) at different population of the high-energy conformer with an assumption of the two-state exchange model. Chemical shift difference $\Delta\omega$, time constant k_{ex} of chemical exchange between the ground state and the transiently populated high-energy state, and a population of the high-energy state p_E were all obtained from the literature (6). Chemical shifts of the ground state of L99A were collected from $^{1}H/^{13}C$-HSQC spectrum obtained at 3 MPa and 25 ^{o}C (Fig. 1*a*). Several residues (I78δ_1 and A99β which belong to the rapid decaying group and I3δ_1, I29δ_1, L46δ_1, L66δ_1, I150δ_1 which belong to the intermediate decaying group) are excluded from this analysis because the parameters for line-shape simulations ($\Delta\omega$, k_{ex} and p_E) were not obtained in the previous NMR ^{13}C-R_2 dispersion experiment (6). The program WINDNMR-Pro was used for the simulations.

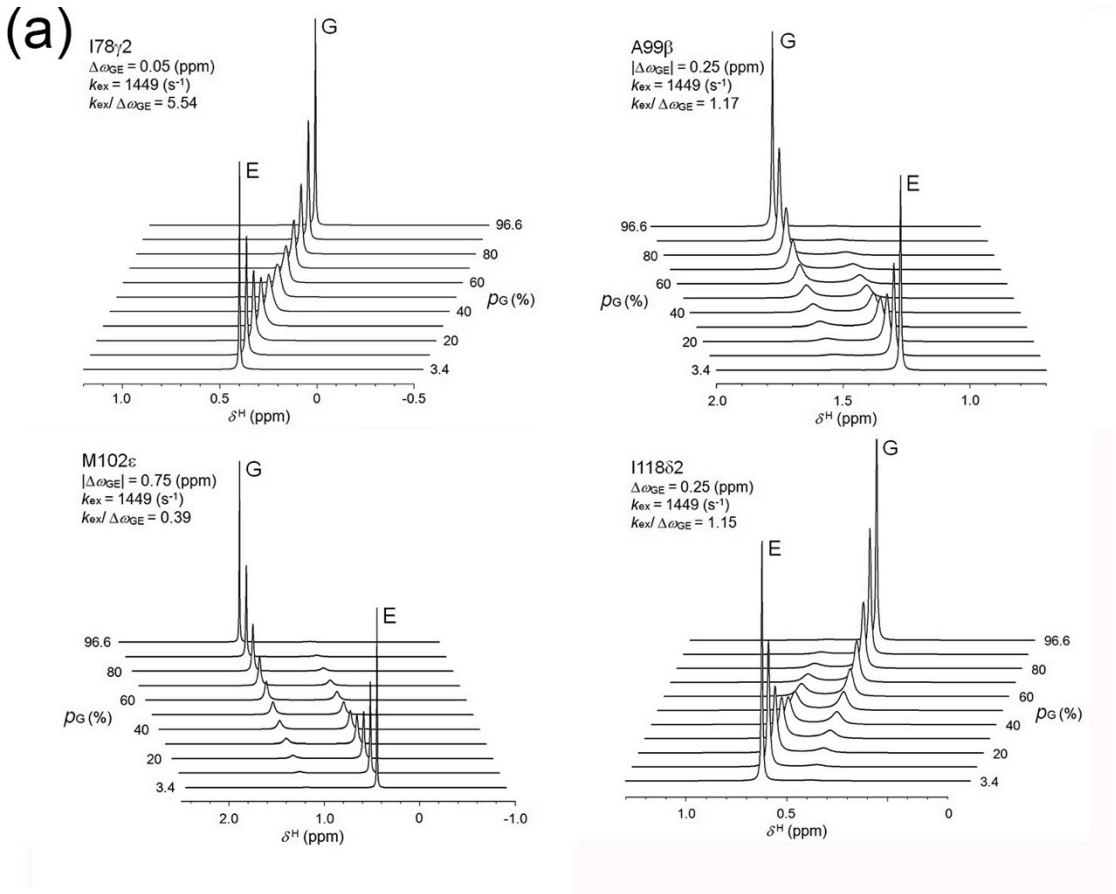
(a)
I78γ2
Δω_GE = 0.05 (ppm)
k_ex = 1449 (s-1)
k_ex/ Δω_GE = 5.54
G
E
96.6
80
60
40
20
3.4
p_G (%)
1.0
0.5
0
-0.5
δ^H (ppm)
A99β
|Δω_GE| = 0.25 (ppm)
k_ex = 1449 (s-1)
k_ex/ Δω_GE = 1.17
G
E
96.6
80
60
40
20
3.4
p_G (%)
2.0
1.5
1.0
δ^H (ppm)
M102ε
|Δω_GE| = 0.75 (ppm)
k_ex = 1449 (s-1)
k_ex/ Δω_GE = 0.39
G
E
96.6
80
60
40
20
3.4
p_G (%)
2.0
1.0
0
-1.0
δ^H (ppm)
I118δ2
Δω_GE = 0.25 (ppm)
k_ex = 1449 (s-1)
k_ex/ Δω_GE = 1.15
G
E
96.6
80
60
40
20
3.4
p_G (%)
1.0
0.5
0
δ^H (ppm)

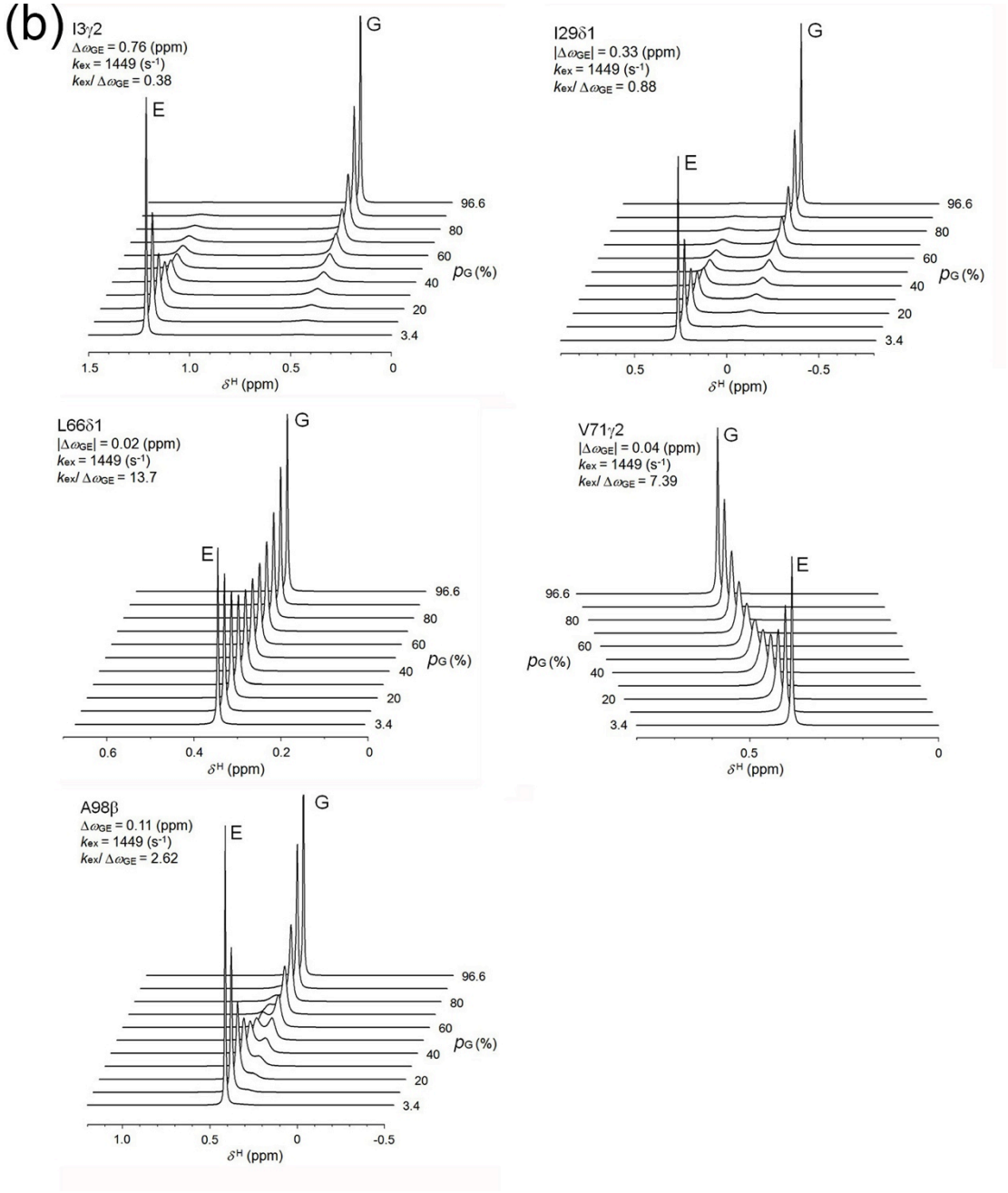

Fig. S5. Line-shape simulation for the methyl protons of L99A involved in (*a*) the rapidly decaying group (e.g. I78Hγ_2, A99Hβ, M102Hε, and I118Hδ_2) and (*b*) the intermediate decaying group (e.g. I3Hγ_2, I29Hδ_1, L66Hδ_1, V71Hγ_2, and A98Hβ) at different population of the high-energy conformer with an assumption of the two-state exchange model. Chemical shift differences $\Delta\omega$ between the ground state and the high-energy state of the L99A/G113A mutant were used in the simulation.

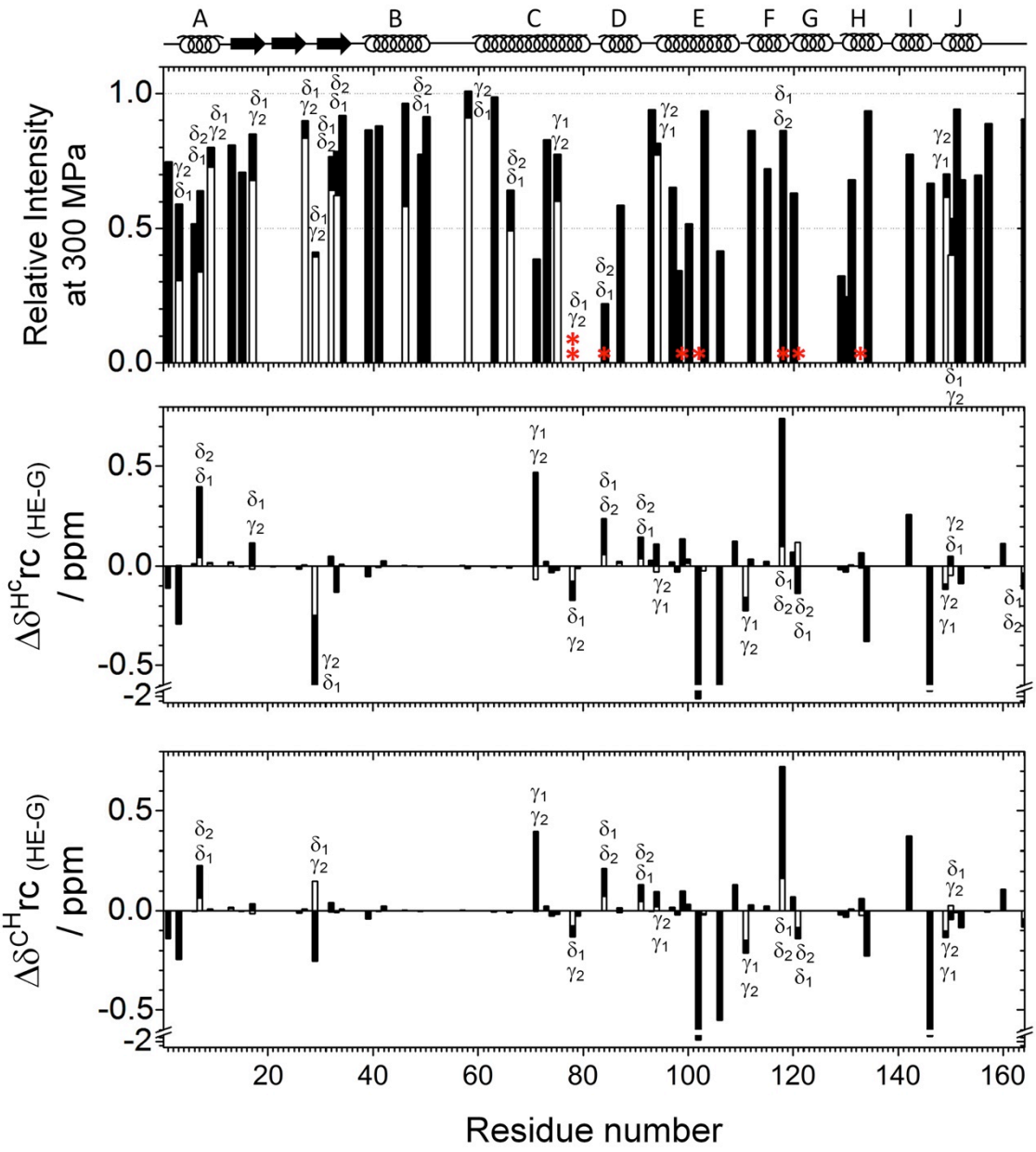

Fig. S6. (*a*) The relative intensities of $^{1}H/^{13}C$ HSQC cross-peaks for L99A at 300 MPa, normalized by those at 0.1 MPa, alongside residue number. Methyl groups showing zero intensity at 300 MPa are marked by asterisks. Secondary structures are represented at the top of each panel (rings for α-helix, arrows for β-stand). Dotted lines show a relative intensity of 0.5. (*b*) Differences of ^{1}H (*top*) and ^{13}C (*bottom*) ring current shifts between the ground (G) and high-energy (HE) states ($\Delta\delta_{rc}$) for the methyl groups along with the residue number. Residues showing remarkable changes are shown by residue numbers. When the residue has two methyl groups, the group indicated at the bottom shows a larger absolute value than the top.

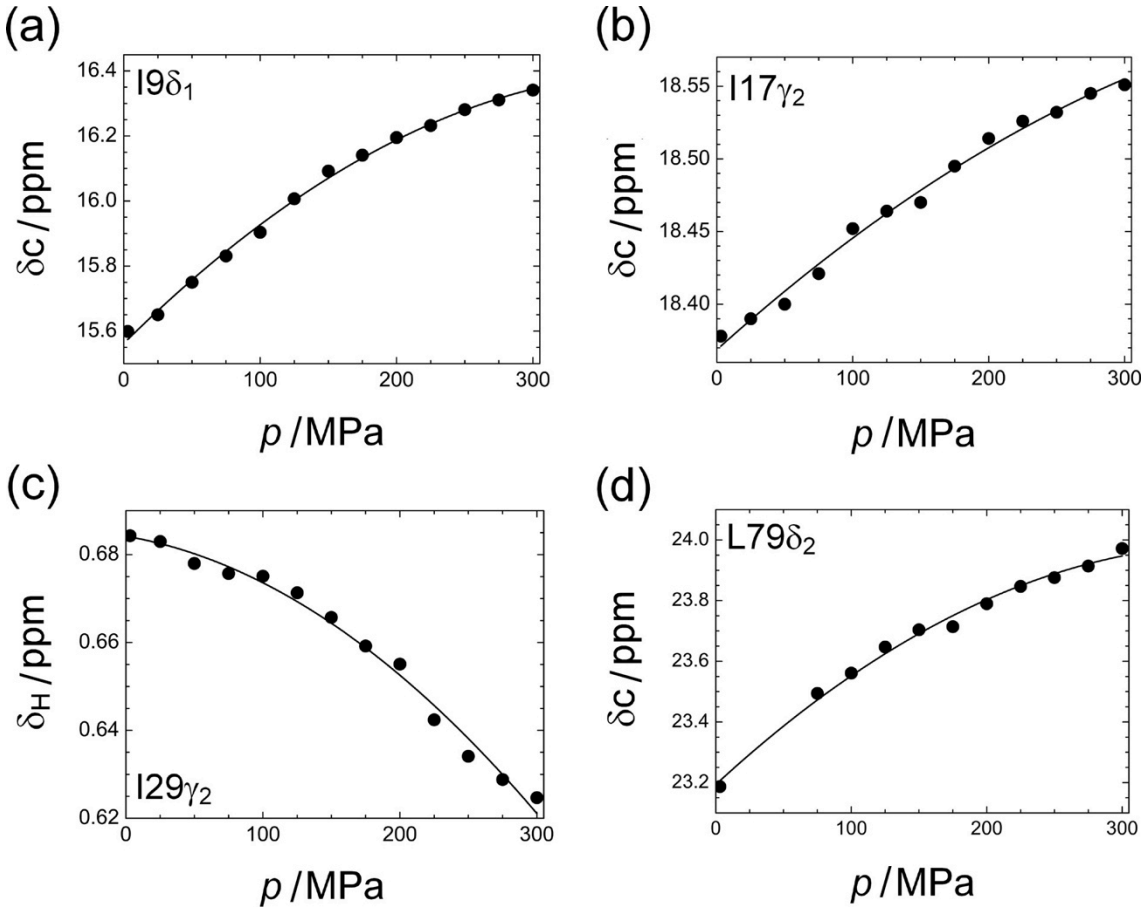

Fig. S7. Non-linear pressure-induced chemical shifts changes for I9 Cδ_1 (*a*), I17 Cγ_2 (*b*), I29 Hγ_2 (*c*), and L79 Cδ_2 (*d*). Some data for L79δ_2 are missing because of peak overlap.

Supporting References

1. Beglov, D., and B. Roux. 1997. An integral equation to describe the solvation of polar molecules in liquid water. *J. Phys. Chem.* B 101:7821-7826.
2. Yoshida, N., T. Imai, S. Phongphanphanee, A. Kovalenko, and F. Hirata. 2009. Molecular recognition in biomolecules studied by statistical mechanical integral-equation theory of liquids. *J. Phys. Chem. B,* 113:873-886.
3. Yokogawa, D., H. Sato, and S. Sakaki. 2009. The position of water molecules in Bacteriorhodopsin: A three-dimensional distribution function study. *J. Mol. Liq.*

147:112-116.

4. Sindhikara, D. J., N. Yoshida, and F. Hirata. 2012. Placevent: An algorithm for prediction of explicit solvent atom distribution: Application to HIV-1 protease and F-ATP synthase. *J. Comput. Chem.* 33:1536-1543.
5. Kovalenko ,A., and F. Hirata. 1998. Three-dimensional density profiles of water in contact with a solute of arbitrary shape: A RISM approach. *Chem. Phys. Lett.* 290:237-244.
6. Mulder, F. A. A., B. Hon, A. Mittermaier, F. W. Dahlquist, L. E. Kay. 2002. Slow internal dynamics in proteins: Application of NMR relaxation dispersion spectroscopy to methyl groups in a cavity mutant of T4 lysozyme. *J. Am. Chem. Soc*. 124:1443-1451.